Edouard *et al.*
The Egyptian Journal of Otolaryngology 2022, **38**(1):111
https://doi.org/10.1186/s43163-022-00301-2

The Egyptian Journal of Otolaryngology

ORIGINAL ARTICLE Open Access

Radiological anatomy of foramen rotundum and its surgical implications

Amani Edouard, Ahmad Aly Ibrahim, Sherif Abdelmoneim Shama, Mostapha Mohamed Abdelnabi, Patrick Balungwe Birindwa and Samy Elwany*

Abstract

Introduction: The use of endoscopic sinus surgery in the field of otorhinolaryngology is due to many reasons such as better visualization, the complex anatomy of the skull base and the relations between vital vascular and nervous elements, the crucial preoperative knowledge about the detailed anatomy of the area, and the computed tomography that is a useful tool for them to plan the safest route of surgery. The foramen rotundum (FR) is the inherent bony structure in the skull base located in the greater wing of the sphenoid bone on the floor of the middle cranial fossa, located adjacent to the nasopharynx, and often invaded by nasopharyngeal cancer and other malignant brain tumors. The This study aims to give a detailed description of anatomical variations of FR, as well as its relationships with the surrounding vital structures, to instruct a preoperative planning for endoscopic surgery.

Methods: The distances between the foramen rotundum and fixed anatomical landmarks like the nasal floor and pterygoid process were measured in 200 foramen rotunda of 100 patients older than 18 years old and without known skull base pathology. The patients included in this study were demonstrated and evaluated separately using a multislice computed tomography (CT) technique with DICOM viewing software (Osirix or Horos).

Results: The average horizontal distance between the FR and vidian canal (VC) on each side, vertical distance between FR and VC on each side, direct distance between the FR and VC on each side, FR diameter, rotundum angles, FRs and nasal floor angles, and FR and optic nerve distances calculated has no significant difference. The *P* values were 0.471, 0.521, 0.072, 0.283, 0.952, 0.661, and 0.663, respectively. The gender comparison in the present study showed no significant distances on both the right and left sides. The *P* values 0.765, 0.879, 0.621, 0.297, 0.992, and 0.227 were direct, horizontal, and direct distances, respectively.

Conclusions: This study provides more light on the anatomy of the foramen rotundum with the other anatomical/surgical key structures used in endonasal surgeries such as the lateral pterygoid plate and vidian canal.

Keywords: Foramen rotundum, Trigeminal nerve, Vidian canal, Optic nerve

Background

Endoscopic sinus operation has been a lot used within the area of otorhinolaryngology due to several reasons including better visualization, minimum invasiveness, and low rate of complications compared to open surgery [1]. The nasal trans-sphenoidal or the extended trans-sphenoidal surgical operation technique is employed by an increasing number of surgeons for approaches of the pterygopalatine fossa, optic canal, internal carotid artery, vidian canal, and clival region [2]. However, the complicated anatomy of the skull base with the relations between important vascular and nervous elements makes this approach challenging for endoscopic surgeons; on the other side, the preoperative information regarding the detailed anatomy of the area is important [1]. The computed tomography could be a useful tool

*Correspondence: samy.elwany@alexmed.edu.eg; samyelwany@msn.com

Alexandria Medical School, Alexandria University Faculty of Medicine, Alexandria, Egypt

for them to set up the safest route of surgery, in order to avoid dramatic complications, like vascular or nervous injury [3].

Foramen rotundum is an inherent bony structure within the skull base located in the greater wing of the sphenoid bone on the floor of the middle cranial fossa; the second or maxillary division of the trigeminal nerve is transmitted through it. FR is located nearby nasopharynx and sometimes invaded by the nasopharyngeal neoplasm and other brain tumors [4].

The FR proximity to pterygopalatine fossa, pterygoid canal, and palatovaginal canal makes it closely related to the transphenoid and the extended transphenoid sinus surgery. Thus, FR is considered as an important landmark [5].

Recently, the event of the endoscopic surgery has made it possible about the structures nearby sphenoid sinus like the internal carotid artery, optic canal, pterygopalatine fossa, and maxillary antrum to obtain access to the FR region. In addition, the maxillary nerve block inside the FR is related to its position [6]. Its precise analysis is difficult and necessitates an adapted technique and also a precise knowledge of its anatomical relationships [7]. The FR is 3.4-mm long and forms a communication between the mid-cranial fossa and the pterygo palatine fossa [4, 8].

The first description of endoscopic endonasal transpterygoid approaches (EETA) aimed to provide access to the lateral sphenoid sinus recess. Surgery techniques and technological resource advancement in the field of endoscopy have permitted the use of EETA to access the foramen lacerum, petrous ICA, Meckel's cave, cavernous sinus, lateral nasopharynx (fossa of Rosenmuller), and ITF [9, 10].

The corridor implied by EETA transgresses the pterygoid process. The two pterygoid processes have medial and lateral plates that go down perpendicularly from the sphenoid bone body part. These plates are fused at the anterior cephalic aspect, the base process of pterygoid. From a ventral aspect, this area contains three useful foramina located from inferomedial to superolateral: palatovaginal canal, vidian canal, and foramen rotundum [10].

Due to the important anatomical relationships, ITF (lateral), PPF (anterior), Eustachian tube and fossa of Rosenmuller (posterior), and middle cranial fossa (superior), a partial or complete removal of the pterygoid process (i.e., transpterygoid approach) is a common step to an endonasal endoscopic access to the infratemporal, middle, and posterior cranial fossa [10].

Aim of the work

The aims of this study give the detailed description of anatomical variations of FR, as well as its relationships with the surrounding vital structures, to instruct preoperative planning for endoscopic surgery.

Methods

The ethical approval was obtained from the Local Ethics Committee of Alexandria University (Decision date: April 4, 2021, serial number: 0106767) before the study has started.

A descriptive approach was adopted for this study of 200 foramen rotunda of 100 patients older than 18 years old and without known skull base pathology. Patients included in this study were demonstrated and evaluated separately using a multislice CT technique. A non-contrast thin-collimation overlapping helical cuts with a maximum section thickness of 0.6mm, and interval of 0.3mm, were performed. Scans were reconstructed in the axial, coronal, and sagittal planes by using high-resolution algorithm bone windows. Images DICOM (digital imaging and communications in medicine) data were transferred to an offline post-processing workstation with a DICOM viewing software (Osirix or Horos).

Data were fed to the computer and analyzed using IBM SPSS software package version 20.0. (Armonk, NY: IBM Corp). Qualitative data were described using a number and percent. The used tests were chi-square test, Monte-Carlo correction, Student's *t* test, Mann-Whitney test, paired *t* test, Wilcoxon-signed ranks test, marginal, and homogeneity test (Figs. 1, 2 and 3).

The following measurements were taken: distance between the anterior nasal spine and foramen rotundum both sides, distance between the right and left foramen rotunda, drawn from the medial wall of one foramen rotundum to another, distances from the midline to the right and left foramen rotundum, distance between the foramen rotundum and the optic nerve on each side; horizontal distance between the foramen rotundum and the vidian canal on each side; vertical distance between the foramen rotundum and the vidian canal on each side; distance between the foramen rotundum and the vidian canal on each side; angle between the foramen rotundum and nasal floor; foramen rotundum diameter, right and left rotundum angles; and foramen rotundum types.

The three types of FR are defined as the follows: *Type I*, when FR is placed completely within the sinus cavity; *Type IIa*, when a part of FR is partially protruding into the SS; *Type IIb*, when FR is tangent to the sinus wall; and *Type III*, when FR is completely placed within the sphenoid bone.

In foramen rotundum positions, regarding the base of the lateral pterygoid plate, the position of the FR is

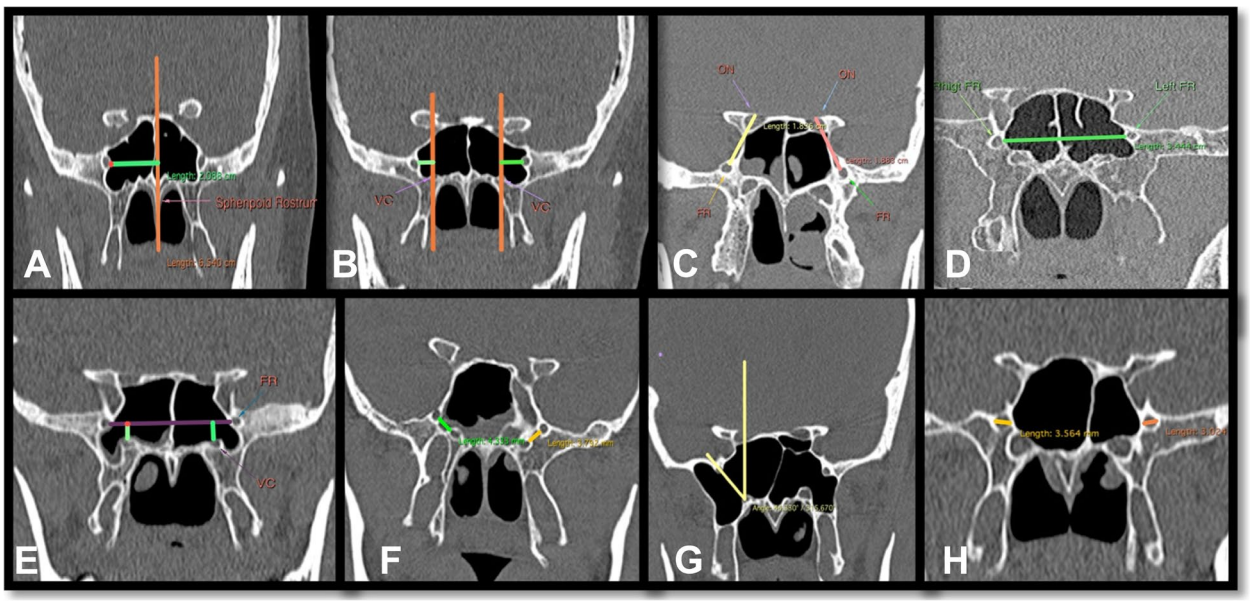

Fig. 1 First measurements. **A** Right distance between right FR to midline, **B** horizontal distance between FR and VC, **C** distance between FR and ON, **D** direct distance between FRs, **E** vertical distance between FR and VC, **F** direct distance between FR and VC, **G** direct distance between FR and VC, **G** rotundum angle, **H** FR diameter

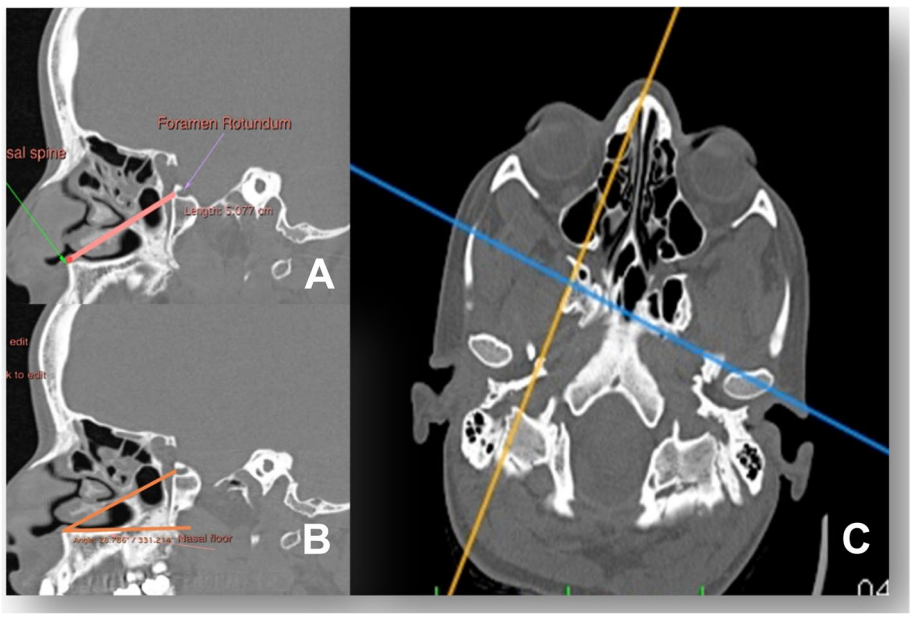

Fig. 2 Second measurements. **A** Distance between FR and nasal spine (NS), **B** angle between FR and nasal floor (NF), and **C** oblique image used to get measurements

defined as *Online*, FR is tangent to the lateral pterygoid plate (midline); *Medial*, FR is medially placed regarding the lateral pterygoid plate; *Lateral*, FR is laterally placed regarding the lateral pterygoid plate.

Results

A total number of one hundred subjects, fourty-seven males (47%) and fifty-three females (53%) ranged from 18 to 72 with a mean age of 38±14.51 years. The mean

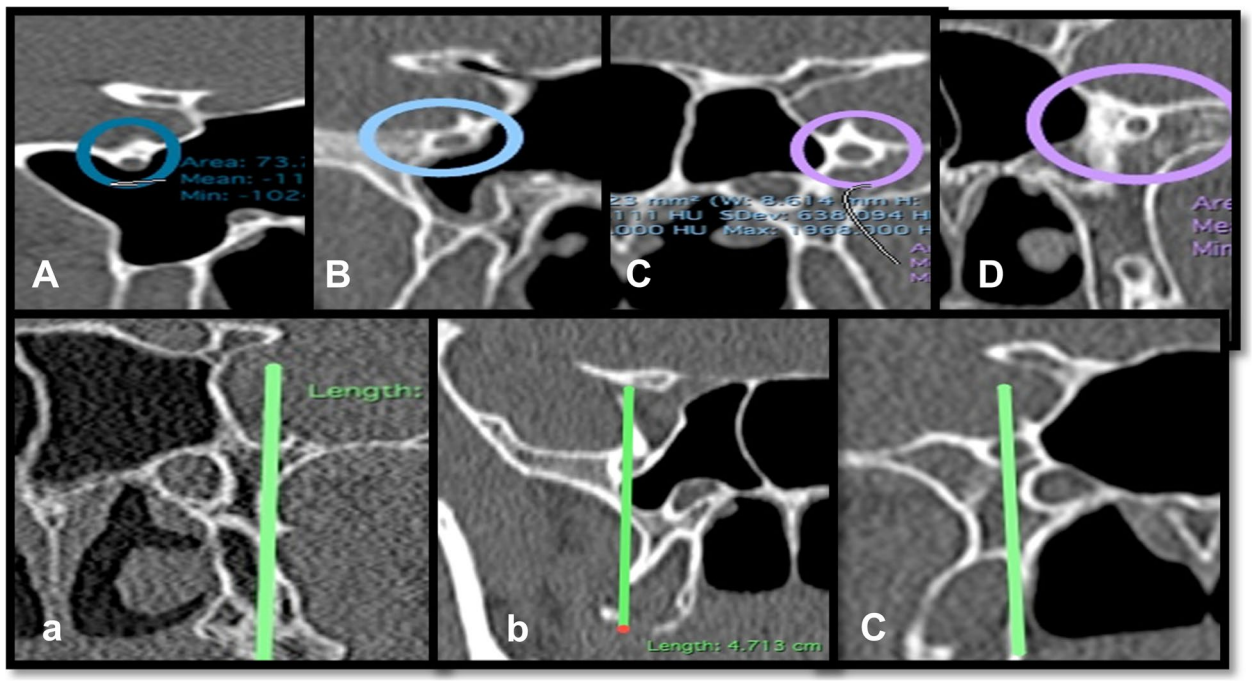

Fig. 3 Types and positions of foramen rotundum. **A** Type I, **B** type IIa, **C** type IIb, **D** type III, **a** left online position, **b** right lateral position, and **c** right medial position

bilateral FR distance according to gender was 3.55 ± 0.38 cm for male and 3.44 ± 0.300 cm for female (*P* value > 0.05) Table 1.

The average horizontal distance between FR and VC each side, vertical distance between FR and VC each side, direct distance between the FR and VC each side, FR diameter, rotundum angles, FRs and nasal floor angles, and FR and optic nerve distances calculated has no significant difference; *P* values were respectively 0.471, 0.521, 0.072, 0.283, 0.952, 0.661, and 0.663. On the other hand, the distance from FR to the midline was significantly wider on the left side compared to the right side and the same for the distance from the anterior nasal spine to FR (*P* values were <0.001 and 0.048), respectively. The types and positions of FRs were not significant on either the right or left side (*P* values of 0.758 and 0.139, respectively) Table 2.

The mean distance of the right FR to the midline was statistically large of 1.75±0.23cm for male compared to females of 1.670±0.18cm (*P* value 0.046) and left side of 1.80±0.17cm compared to the right side of 1.83±0.26cm (*P* value < 0.001). The horizontal calculated

Table 1 Comparison between the right side and left side according to different variables in total sample

	Right side ($n = 100$)	Left side ($n = 100$)	Test of sig.	*P*
FR distance to the midline (cm)	1.71 ± 0.21	1.81 ± 0.22	Z=4.185*	<0.001*
Horizontal distance FR to VC (mm)	4.61 ± 1.62	4.73 ± 1.64	t=0.723	0.471
Vertical distance FR to VC (mm)	3.99 ± 1.80	4.12 ± 1.89	Z=0.641	0.521
Direct distance FR to VC (mm)	5.40 ± 2.25	5.71 ± 2.39	t=1.817	0.072
Diameter of FR (mm)	3.15 ± 0.55	3.15 ± 0.79	Z=1.073	0.283
FR angle (degree)	47.51 ± 10.65	47.57 ± 9.51	t=0.060	0.952
Distance between anterior nasal spine to FR (cm)	6.22 ± 0.46	6.30 ± 0.50	t=2.001*	0.048*
Angle between nasal floor and FR (degree)	29.13 ± 6.56	29.37 ± 5.76	t=0.440	0.661
Distance between optic nerve and FR (cm)	1.74 ± 0.20	1.75 ± 0.19	t=0.437	0.663

SD standard deviation, *t* paired *t* test, *Z* Wilcoxon-signed ranks test

*Statistically significant at $P \leq 0.05$. *FR* foramen rotundum, *VC* vidian canal

Table 2 Comparison between male and female according to different measurements in each side

		Sex		Test of Sig	*P*
		Male ($n = 47$)	**Female ($n = 53$)**		
FRML (cm)	**Right side**				
	Min.–Max.	1.20–2.17	1.27–2.0	U=956.0*	0.046*
	Mean ± SD.	1.75 ± 0.23	1.67 ± 0.18		
	Median (IQR)	1.79 (1.61–1.91)	1.70 (1.53–1.82)		
	Left side				
	Min.–Max.	1.22–2.70	1.48–2.21	U=1142.5	0.477
	Mean ± SD.	1.83 ± 0.26	1.80 ± 0.17		
	Median (IQR)	1.83 (1.71–1.96)	1.80 (1.68–1.89)		
	Z (p_0)	1.730 (0.084)	4.177* (<0.001*)		
HOR-FRVC (mm)	**Right side**				
	Min.–Max.	1.68–8.94	1.80–8.26	t=0.495	0.621
	Mean ± SD.	4.53 ± 1.52	4.69 ± 1.72		
	Median (IQR)	4.45 (3.37–5.38)	4.35 (3.32–5.92)		
	Left side				
	Min.–Max.	1.65–9.01	1.41–10.0	t=1.049	0.297
	Mean ± SD.	4.55 ± 1.54	4.90 ± 1.73		
	Median (IQR)	4.59 (3.37–5.43)	4.48 (3.70–5.97)		
	t_0 (p_0)	0.084 (0.933)	0.947 (0.348)		
VERT-FRVC (mm)	**Right side**				
	Min.–Max.	0.50–7.62	0.70–8.45	U=1244.0	0.992
	Mean ± SD.	3.90 ± 1.56	4.08 ± 2.01		
	Median (IQR)	3.63 (2.72–4.63)	3.76 (2.64–5.86)		
	Left side				
	Min.–Max.	1.31–9.39	1.0–8.47	U=1070.5	0.227
	Mean ± SD.	3.92 ± 1.84	4.31 ± 1.93		
	Median (IQR)	3.65 (2.52–5.02)	4.30 (2.80–5.43)		
	Z (p_0)	0.085 (0.933)	1.053 (0.292)		
DD-FRVC (mm)	**Right side**				
	Min.–Max.	1.31–10.0	0.77–12.0	t=0.299	0.765
	Mean ± SD.	5.47 ± 2.04	5.34 ± 2.44		
	Median (IQR)	5.40 (3.82–7.05)	4.69 (3.73–7.17)		
	Left side				
	Min.–Max.	1.30–10.50	1.0–11.60	t=0.153	0.879
	Mean ± SD.	5.67 ± 2.56	5.74 ± 2.25		
	Median (IQR)	5.60 (3.50–7.30)	5.64 (4.40–7.55)		
	t_0 (p_0)	0.703 (0.486)	2.004* (0.050*)		
FR-DMT (mm)	**Right side**				
	Min.–Max.	2.0–4.51	1.44–4.15	U=950.0*	0.041*
	Mean ± SD.	3.27 ± 0.59	3.05 ± 0.49		
	Median (IQR)	3.36 (2.82–3.70)	3.0 (2.84–3.37)		
	Left side				
	Min.–Max.	1.29–7.28	1.88–4.31	U=919.0*	0.024*
	Mean ± SD.	3.35 ± 0.97	2.97 ± 0.55		
	Median (IQR)	3.20 (2.84–3.56)	2.94 (2.62–3.24)		
	Z (p_0)	0.482 (0.630)	1.070 (0.285)		

SD standard deviation, *IQR* interquartile range, *t* Student's *t* test, *U* Mann-Whitney *U* test, t_0 paired *t* test, *Z* Wilcoxon-signed ranks test

* Statistically significant at $P \leq 0.05$, *FR-DMT* foramen rotundum diameter, *DD-FRVC* direct distance foramen rotundum to vidian canal, *VERT-FRVC* vertical distance foramen rotundum to vidian canal, *HOR-FRVC* horizontal distance foramen rotundum to vidian canal; *FRML* distance foramen rotundum to midline

statistical distances between FR and VC were not significant between genders with *P* values 0.621 and 0.297 on the right and the left sides, respectively, and between sides with *P* values 0.933 and 0.348 for male and female, respectively. Tables 3 presents all the details concerning the distances between FRs and VCs, and rotundum diameters according to gender and sides. Table 4 shows the measurements of the rotundum angles crossing between sides and genders, the angle between the FR and the anterior nasal spine, and the distance between the FR and the optic nerve.

Table 5 presents details on the types and positions of FRs according to gender and sides.

Discussion

The literature is lacking of profound anatomical descriptions of this complex area. It is primordial to obtain this anatomical knowledge in order to achieve efficiency and

Table 3 Comparison between male and female according to different measurements in each side

		Sex		Test of sig	*p*
		Male (*n* = 47)	**Female (*n* = 53)**		
FR angle (degree)	**Right side**				
	Min.–Max.	22.50–74.35	25.30–75.80	*t*=0.732	0.466
	Mean ± SD.	48.34 ± 11.46	46.77 ± 9.94		
	Median (IQR)	49.0 (39.0–54.8)	45.90 (41.1–52.3)		
	Left side				
	Min.–Max.	29.40–69.60	28.10–72.19	*t*=0.012	0.991
	Mean ± SD.	47.56 ± 9.20	47.58 ± 9.88		
	Median (IQR)	48.0 (40.8–54.0)	47.20 (40.9–53.8)		
	t_0 (p_0)	0.457 (0.650)	0.592 (0.557)		
NFFR angle (degree)	**Right side**				
	Min.–Max.	2.20–45.60	18.56–40.60	*t*=0.287	0.775
	Mean ± SD.	28.93 ± 8.08	29.31 ± 4.90		
	Median (IQR)	29.30 (25.3–32.5)	29.70 (26.4–32.5)		
	Left side				
	Min.–Max.	17.60–40.40	15.20–47.50	*t*=0.462	0.645
	Mean ± SD.	29.65 ± 5.43	29.12 ± 6.08		
	Median (IQR)	29.80 (25.8–33.6)	29.30 (25.6–32.4)		
	t_0 (p_0)	0.792 (0.432)	0.304 (0.762)		
ANS FR (cm)	**Right side**				
	Min.–Max.	5.16–7.27	4.92–7.09	*t*=2.921*	0.004*
	Mean ± SD.	6.36 ± 0.48	6.10 ± 0.40		
	Median (IQR)	6.32 (6.02–6.72)	6.13 (5.87–6.37)		
	Left side				
	Min.–Max.	4.90–7.30	4.42–6.97	*t*=3.259*	0.002*
	Mean ± SD.	6.47 ± 0.56	6.15 ± 0.40		
	Median (IQR)	6.51 (6.24–6.83)	6.20 (5.98–6.33)		
	t_0 (p_0)	1.696 (0.097)	1.074 (0.288)		
ONFR distance (cm)	**Right side**				
	Min.–Max.	1.33–2.34	1.22–2.07	*t*=2.130*	0.036*
	Mean ± SD.	1.78 ± 0.20	1.70 ± 0.20		
	Median (IQR)	1.79 (1.67–1.90)	1.69 (1.57–1.80)		
	Left side				
	Min.–Max.	1.29–2.17	1.36–2.17	*t*=0.972	0.333
	Mean ± SD.	1.77 ± 0.19	1.73 ± 0.20		
	Median (IQR)	1.76 (1.66–1.88)	1.71 (1.61–1.86)		
	t_0 (p_0)	0.796 (0.430)	1.280 (0.206)		

SD standard deviation, *IQR* interquartile range, *t* Student's *t* test, *U* Mann-Whitney *U* test, t_0 paired *t* test, *Z* Wilcoxon-signed rank test, *ONFR* distance foramen rotundum to optic nerve, *ANS FR* distance foramen rotundum to optic nerve, *NFFR* angle between foramen rotundum and nasal floor, *FR* foramen rotundum

Table 4 Comparison between the right side and left side according to the FR type and FR position in a total sample

	Right side ($n = 100$)		Left side ($n = 100$)		MH	*p*
	No.	%	No.	%		
FR type						
Type 1	4	4.0	3	3.0	85.0	0.758
Type 2A	12	12.0	19	19.0		
Type 2B	46	46.0	33	33.0		
Type 3	38	38.0	45	45.0		
FR position						
Lateral position	3	3.0	5	5.0	65.50	0.139
Online position	22	22.0	27	27.0		
Medial position	75	75.0	68	68.0		

FR foramen rotundum, *MH* marginal homogeneity test, *p P* value for comparing between the right side and left side

Table 5 Comparison between male and female according to FR type and FR position to the lateral pterygoid plate

		Sex				χ^2	^{MC}p
		Male ($n = 47$)		Female ($n = 53$)			
		No.	%	No.	%		
FR type	**Right side**						
	Type 1	1	2.1	3	5.7	2.643	0.460
	Type 2A	6	12.8	6	11.3		
	Type 2B	25	53.2	21	39.6		
	Type 3	15	31.9	23	43.4		
	Left side						
	Type 1	0	0.0	3	5.7	7.937*	0.034*
	Type 2A	11	23.4	8	15.1		
	Type 2B	20	42.6	13	24.5		
	Type 3	16	34.0	29	54.7		
	MH (p_0)	44.0 (0.655)		41.00 (0.394)			
FR position	**Right side**						
	Lateral position	2	4.3	1	1.9	0.590	0.852
	Online position	10	21.3	12	22.6		
	Medial position	35	74.5	40	75.5		
	Left side						
	Lateral position	2	4.3	3	5.7	1.763	0.410
	Online position	10	21.3	17	32.1		
	Medial position	35	74.5	33	62.3		
	MH (p_0)	22.0 (1.000)		43.50* (0.050*)			

χ^2 chi-square test, *MC* Monte-Carlo, *MH* marginal homogeneity test, *p p* value for comparing between male and female, p_0 *P* value for comparing between the right side and left side

*Statistically significant at $p \leq 0.05$

safety at the endoscopic endonasal approaches of this region. In this study, high-resolution CT was applied to measure the foramen rotundum distances to the contralateral side, midline, vidian canal, optic nerve, rotundum angle, anterior nasal spine, its angle with the floor of the nose, and its positions and types.

The asymmetry found in the distance from FR to the midline axis was compared to some previous studies. Mohebi et al. [9] found to have asymmetrically distances from FR to the midline axis, larger on the left side (19.34 ± 2.17mm) than the right side (19.00 ± 2.07mm) (*P* value 0.03). Kasmsiri et al. [10] have

described the average distance from midline to the left FR as 19.11 mm (SD 2.34 mm) and 17.67 mm to the right FR (SD 1.7) (*P* value 0.046). Gozde Serindere et al. [2] discovered a significant difference in the distance from midline to the right and left FR. The gender calculated measurements showed an asymmetry between the two sides larger for male compared to female on the right side (*P* value 0.048). This serves as important information that can be used by the endoscopic skull base surgeon when trying to safely localize the FR during the approaches through the SS.

In bilateral foramen rotundum distance, Mikail et al. [7] study of 320 coronal CT of adult Japanese in 2015 by using the same methodology reported a significant bilateral foramen rotundum distance between the men and women. Less similar study of Kim et al. [11] has reported that the distance between the foramina rotunda was a little greater in the anterior segment in general.

In the present study, the distance between FR and VC (horizontal, vertical, and direct distances) measurements have shown no significant differences. The *P* values were 0.471, 0.521, and 0.072, respectively. Mohebi et al. [9], have discovered the same results; FR distances to VCs were symmetrical in horizontal, vertical, and direct, and no statistically significant difference ($P = 0.764$, 0.676, and $P = 0.952$, respectively). With the study of Kasmsiri [10], the average horizontal, vertical, and distances from FR to VC reported no significant difference between the right and left sides. According to Gozde et al. [2], there is a significant difference in the distance from the horizontal, vertical, and direct distances from the right and left FRs to VCs.

The gender comparison in the present study showed no significant distance in both right and left sides. The *P* values 0.765, 0.879, 0.621, 0.297, 0.992, and 0.227 are for direct, horizontal, and direct distances, respectively. The same symmetrical distances between genders were measured by Gozde [2] in his study, and the *P* values 0.202, 0.984, 0.217, 0.934, 0.453, and 0.738 are for right and left direct, horizontal, and vertical distances, respectively. This is important as EETs require a corridor that crosses the maxillary sinus or ablates or displaces the soft tissue contents of the PPF and removes partially the pterygoid process or completely to reach and control the surgical fields. The necessary dimensions of this corridor is often difficult to be estimated during the preoperative planning. In order to anticipate the dimensional needs of the corridor, EETAs can be better conceptualized (and estimated preoperatively) by vertical and horizontal imaginary lines that cross the vidian and rotundum foramina, respectively.

The primary trigeminal neuralgia (TN) can occasionally occur without neurovascular compression. Another mechanism than neurovascular compression may play a role in TN, and investigation of potential mechanism by measuring the sizes of the foramen rotundum on high-resolution computed tomography (CT) image, focusing on the primary TN without vascular compression during surgery, may help to rule out all other mechanisms [12].

In Pengfei et al.'s study [12] in the Chinese population, the diameter appeared narrow, with a mean distance of 2.52 ± 0.43mm on the right side and 2.65 ± 0.45mm on the left side, without a statistical difference between the right and the left side (*P* value 0.28). A cadaveric dissection study conducted by Kocaogullar et al. [13] reported an average diameter of FR (3.11mm) in cadaver specimens (3.44mm) in skulls without a statistical significance between the right and left in a study of 52 specimens (cadaver and skull). Also, Nadire Unver Dogan [14], in a study conducted in Turkey, had observed no statistical significance ($P>0.05$) between both sides in the average longitudinal diameters (4.48 ± 1.15 mm in the right, 4.36 ± 0.66 mm in the left) and average transverse diameters but wider in size.

As regards the distribution according to the position of FR regarding the base of lateral pterygoid plate as observed in the table, the FR was online placed in 24.5% of the patients, medially placed in 71.5% of the patients, and in 4% of the total foramens were placed laterally. It is shown from the study that online and medial types are the most common types that is in direct agreement with Mohebbi A. who reported 48%, 50%, and 2%, respectively. Ramanna et al. [15] have presented 50%, 57%, and 3%, online, medially, and laterally placed, respectively. Gozde Serindere observed in his study the same symmetrical results that FR is located 0.570, 0.150, and 0.758 online, medial, and lateral, respectively, located according to gender. This observation may help the better localization of FR in relation to VC and the pterygoid process, in order to facilitate its safe identification and help the surgeon avoid an inadvertent injury to their anatomical integrity.

In the FR position within the sphenoid bone, the present study revealed that the FR was either placed completely within the sinus cavity (type I), 3.5%; a part of FR is in the sinus cavity or partially protruding into the SS (type IIa), 15.5%; FR is tangent to the sinus wall (type IIb), 39.5%; FR is placed completely within the sphenoid bone (type III), 41.5%. Ramanna et al. [15] reported 6%, 32%, 44%, and 18%, respectively. Gozde et al. [2] reported that four patients (4%) had type I FR; 28% and 44% had type IIa and IIb, respectively; and 24% had type III FR. The relations of the SS with surrounding structures are close when the sinus is well pneumatized. The surrounding vessels and nerves are well seen in the sinus cavity as irregularities or ridges. The pneumatization of the

sphenoid to the pterygoid processes is an extension of the sinus between the maxillary nerve and the nerve of the pterygoid canal (vidian nerve) [9].

As regards the rotundum angle, comparing the right to the left FR side among the total population, this showed 47.51±10.65° on the left side and 47.57± 9.51° on the right side. The *P* value was 0.952. Similar with the results with Mohebi et al., 46.76 ± 12.32° is on the right side and 46.40 ± 10.67° on the left side. The *P* value is 0.647. Gozde et al. reported the right rotundum angle *P* value of 0.021 and the left rotundum angle *P* value of 0.275.

The mean distance from the anterior nasal spine to the foramen rotundum was significantly longer in males of 6.36 ± 0.48cm on the right side and 6.47 ± 0.56cm on the left side compared with females (6.10 ± 0.40cm and 6.15 ± 0.40 cm on the right and left sides, respectively). The gender difference was confirmed by *P* values of 0.004 and 0.002, but the difference between right and left was not significant. On coronal CT angiographies of 34 Egyptians, Ahmed et al. [16] found a gender average of 6.98±0.88cm on right side and 6.93±0.887 on left side compared to 6.58±0.488cm on the right side and 6.62±0.436 cm on the left side. The apparently high numbers can be explained by the columella used as landmark instead of anterior nasal spine used in our study.

The foramen rotundum is related intimately to the lateral wall of the sphenoid sinus. The significance of variations is not fully understood, and the maxillary nerve may be more vulnerable to pathological conditions involving the sphenoid sinus [11].

There have been previous descriptions contained within the literature to evaluate the foramen rotundum localization and its relationship to the surrounding endonasal and skull base landmarks, but to our knowledge, the measurements conducted in this study (size of the angle between the floor of the nasal floor and the foramen rotundum) have not been recorded before, and they will provide surgeons with an additional and reliable description to use during operation.

This study has been carried on 100 adult patients (47 males and 43 females) who undergo paranasal sinus (PNS) computed tomography scan (0.6-mm slices thickness) for any reason, in the Otorhinolaryngology Department of Alexandria Main University Hospital. All individuals younger than 18 years of age, or with known skull base pathology and marked facial deformity, were not included.

There were no significant differences between measurements on the right and left sides regarding the mean distance of the horizontal distance between the foramen rotundum and vidian canal on each side, the vertical distance between the foramen rotundum and vidian canal on each side, the direct mean distance between the foramen rotundum and vidian canal on each side, the mean diameter of foramen rotundum on each side, the mean angle of foramen rotundum on each side, the mean angle between nasal floor and the foramen rotundum on each side, and the mean distance between the foramen rotundum and optic nerve on each side; The *P* values were 0.471, 0.521, 0.072, 0.283, 0.952, and 0.661, respectively. On the other hand, the distance from the foramen rotundum to the midline was significantly longer on the left side compared to the right side where the distance from the anterior nasal spine to the foramen rotundum was significantly larger on the left side compared to the right side. The *P* values were <0.001 and 0.048, respectively.

Conclusion

This study provides more light on the anatomy of foramen rotundum with the other anatomical/surgical key structures used in endonasal surgeries such as lateral pterygoid plate and vidian canal. The application of submillimeter, thin-section HRCT scanning, and reconstruction can provide comprehensive details.

The study results will be used by endoscopic skull base surgeons to get an idea on the most common types of anatomical variations of the foramen rotundum which aids in better understanding of this complex area before surgery resulting in better prognosis in the Egyptian population particularly.

Abbreviations

ANS-FR: Distance between the anterior nasal spine and foramen; CN: Cranial nerve; CT: Computer tomography; CSF: Cerebrospinal fluid; DD-FRVC: Direct distance between foramen rotundum and vidian canal; DICOM: Digital imaging and communication; EETA: Endoscopic endonasal transpterygoid approach; FR: Foramen rotundum; FR DM: Foramen rotundum diameter; FR-ML: Distance between foramen rotundum to the midline; HOR-FRVC: Horizontal distance between foramen rotundum and vidian canal; ITF: Infra temporal fossa; ICA: Internal carotid artery; IQR: Interquantile range; LR: Lateral recess; LRSS: Lateral recess of sphenoid sinus; MCF: Midcranial fossa; MRI: Magnetic resonance imaging; NF-FR: Angle between foramen rotundum and nasal floor; OC: Optic canal; ON-FR: Distance between the optic nerve and the foramen rotundum; PPG: Pterygo palatine ganglia; VC: Vidian canal; PICAC: Petrous segment of internal carotid canal; PNS: Paranasal sinus; PPF: Pterygopalatine fossa; RL-FR: Distance between the right and the left foramen rotunda; SD: Standard deviation; SNT: Sinonasal tract; SS: Sphenoid sinus; VERT-FRVC: Vertical distance between foramen rotundum and vidian canal; V1: Ophtalmic nerve; V2: Maxillary nerve; V3: Mandibular nerve.

Acknowledgements

All authors are thankful to the Department of Otolaryngology of the Alexandria University. Amani Mudekereza Edouard, Dr. Ahmad Youssef Sohbi, and Dr. Paterne Safari Mudekereza are thankful to the Hopital Provincial General de Reference de Bukavu, the Universite Catholique de Bukavu.

Authors' contributions

AME, AAI, SAS, MMA, PBB and SE, have designed, conceptualized and made a critical review of the manuscript. AME and AAI wrote the first draft of the manuscript, All authors have reviewed and approved the last version of the paper.

Funding
Not applicable

Availability of data and materials
Not applicable

Declarations

Ethics approval and consent to participate
This work has received the ethical approval from the ethical committee of the Faculty of Medicine of the Alexandria University on April 15, 2021, under serial number: 0106767. Informed written consent to participate in the study was provided by all participants.

Consent for publication
Not applicable

Competing interests
The authors declare that they have no competing interests.

Received: 21 June 2022 Accepted: 3 July 2022
Published: 29 August 2022

References

1. Turkdogan FT, Turkdogan KA, Dogan M, Atalar MH (2017) Assessment of sphenoid sinus related anatomic variations with computed tomography. Pan Afr Med J 27:1–7
2. Serindere G, Gunduz K, Avsever H (2020) The measurement indexes and the relationships with adjacent structures of vidian canal and foramen rotundum using computed tomography. J Anat Soc India 69(3):144–149
3. Vaezi A, Cardenas E, Pinheiro-Neto C, Paluzzi A, Branstetter BF, Gardner PA et al (2015) Classification of sphenoid sinus pneumatization: relevance for endoscopic skull base surgery. Laryngoscope. 125(3):577–581
4. Ginsberg LES, Pruett SW, Chen MYM, Elster AD (1994) Skull-base foramina of the middle cranial fossa: reassessment of normal variation with high-resolution CT. Am J Neuroradiol 15(2):283–291
5. Edwards B, Wang JM, Iwanaga J, Loukas M, Tubbs RS (2018) Cranial Nerve Foramina Part I: A Review of the Anatomy and Pathology of Cranial Nerve Foramina of the Anterior and Middle Fossa. Cureus 10(2):e2172. https://doi.org/10.7759/cureus.2172. PMID: 29644159; PMCID: PMC5889149
6. Cömert S, Kontzialis M (2021) Foramen rotundum duplication on high-resolution Ct. case report. SN Compr Clin Med 3(2):692–693
7. Inal M, Muluk NB, Arikan OK, Şahin S (2015) Is there a relationship between optic canal, foramen rotundum, and vidian canal? J Craniofac Surg 26(4):1382–1388
8. Unver Dogan N, Fazliogullari Z, Uysal II, Seker M, Karabulut AK (2014) Anatomical examination of the foramens of the middle cranial fossa. Int J Morphol 32(1):43–48
9. Mohebbi A, Rajaeih S, Safdarian M, Omidian P (2017) The sphenoid sinus, foramen rotundum and vidian canal: a radiological study of anatomical relationships. Braz J Otorhinolaryngol 83(4):381–387
10. Kasemsiri P, Solares CA, Carrau RL, Prosser JD, Prevedello DM, Otto BA et al (2013) Endoscopic endonasal transpterygoid approaches: anatomical landmarks for planning the surgical corridor. Laryngoscope. 123(4):811–815
11. Kim HS, Kim DI, Chung LH, Kim) H S, Chung IH. (1996) High-resolution CT of the pterygopalatine fossa and its communications. Neuroradiology 38
12. Liu P, Zhong W, Liao C, Liu M, Zhang W (2016) Narrow foramen ovale and rotundum: a role in the etiology of trigeminal neuralgia. J Craniofac Surg 27(8):2168–2170
13. Kocaoğullar Y, Avci E, Fossett D, Caputy A (2003) The extradural subtemporal keyhole approach to the sphenocavernous region: anatomic considerations. Minim Invasive Neurosurg 46(2):100–105
14. Unver Dogan N, Fazliogullari Z, Uysal II, Seker M, Karabulut AK (2014) Anatomical examination of the foramens of the middle cranial fossa. Int J Morphol 32(1):43–48 Mar [cited 2022 Feb 10]
15. Ramanna HC, Gowda SS, Jithendra N, Vijay Kumar KR (2020) A radio-anatomic profile of the sphenoid sinus, vidian canal and foramen rotundum structured. J Evid Based Med Heal thc 7(40):2294–2299
16. Youssef A, Carrau RL, Tantawy A, Ibrahim AA, Prevedello DM, Otto BA et al (2014) Clinical correlates of the anatomical relationships of the foramen ovale: a radioanatomical study. J Neurol Surgery, Part B Skull Base 75(6):427–434

Publisher's Note